Electronic Supplementary Material (ESI) for Journal of Materials Chemistry A.

Supporting Information

Balancing Stability and Specific Energy in Li-Rich Cathodes for Lithium Ion Batteries: A Case Study of a Novel Li-Mn-Ni-Co Oxide

*Qi Li, Guangshe Li, Chaochao Fu, Dong Luo, Jianming Fan, Dongjiu Xie and Liping Li**

Key Laboratory of Design and Assembly of Functional Nanostructures, Fujian Institute of Research on the Structure of Matter, Chinese Academy of Sciences, Fuzhou 350002, PR China

E-mail: lipingli@fjirsm.ac.cn

I. Morphology observation of carbonate precursor

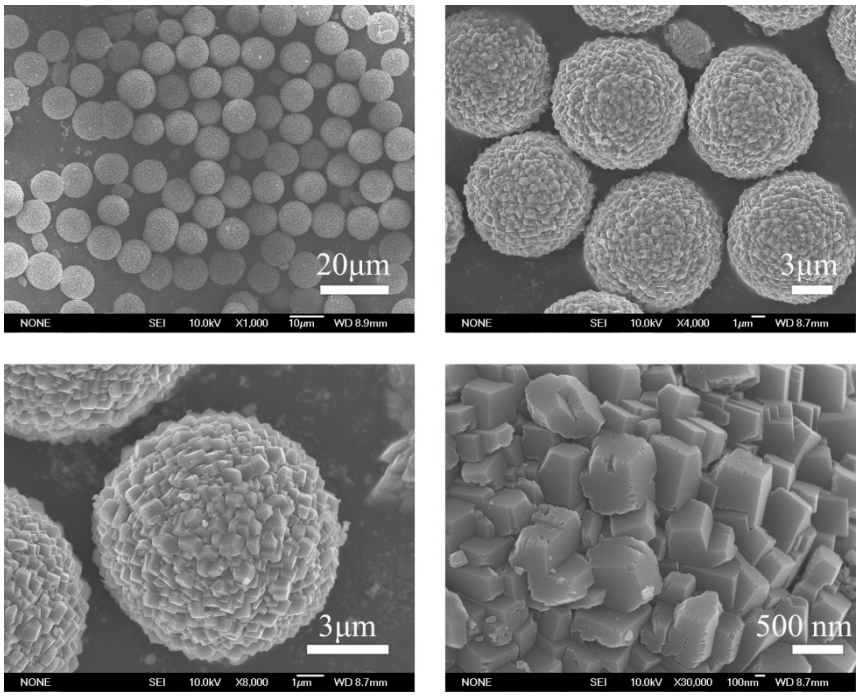

Figure S1. SEM images of carbonate precursor prepared via a solvo/hydro-thermal method.

II. Structural analysis of $Li_{1.08}Mn_{0.503}Ni_{0.387}Co_{0.03}O_2$

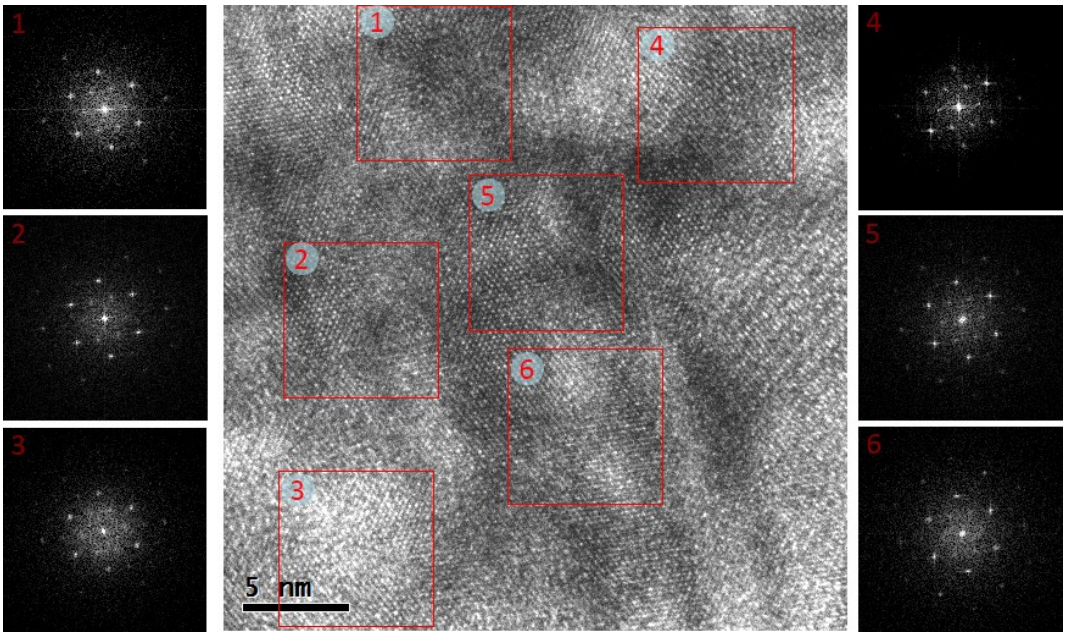

Figure. S2 Probing local structures of $Li_{1.08}Mn_{0.503}Ni_{0.387}Co_{0.03}O_2$: different local domains and corresponding Fast Fourier Transformation (FFT) patterns.

Six different *ca.* 7 nm x 7 nm domains locating in the same area with that in Figure 2 are marked and their FFT patterns are shown in Figure S2. Intensity of the inside diffraction dots, which are assigned to *C2/m* phase, show clear discrepancies in different regions. This might indicate that inhomogeneity exists in local domains, which could be due to phase segeration between $LiMO_2$- and Li_2MnO_3-like phases in this compound. A supplymentary evidence is from EDS data at two random area, which show different Ni/Mn ratio. Note again that this just a possible but not conclusive proof in favor of composite structure.

III. Comparision of the performance parameters for various commercialized cathodes

Table S1. Best-case (low rate), practically achievable, working voltages and capacities versus Li/Li^+ for various cathode materials*

Material	Working voltage (ave. *vs.* Li^+/Li)	Capacity (mAh/g)	Specific energy (Wh/kg)
$LiCoO_2$(LCO)	3.8	150	570
$LiNi_{1/3}Mn_{1/3}Co_{1/3}O_2$(NCM)	3.7	170	629
$LiNi_{0.8}Co_{0.15}Al_{0.05}O_2$(NCA)	3.7	185	685
$LiMn_2O_4$	4.0	110	440
$LiFePO_4$(LFP)	3.4	160	544
$LiMn_{1.5}Ni_{0.5}O_4$	4.7	135	635
This Work	**3.9**	**210**	**805**

*The reference data are collected from ref. [1].

Table S1 summarizes the best-case parameters of various commercialized cathode materials, tabulated along with the corresponding values for the layered oxide reported in this work. The comparison aims to illustrate the superior energy density and high working voltage than commercial materials. To visually reach this point, the Table is converted into bar graphs in Figure S2.

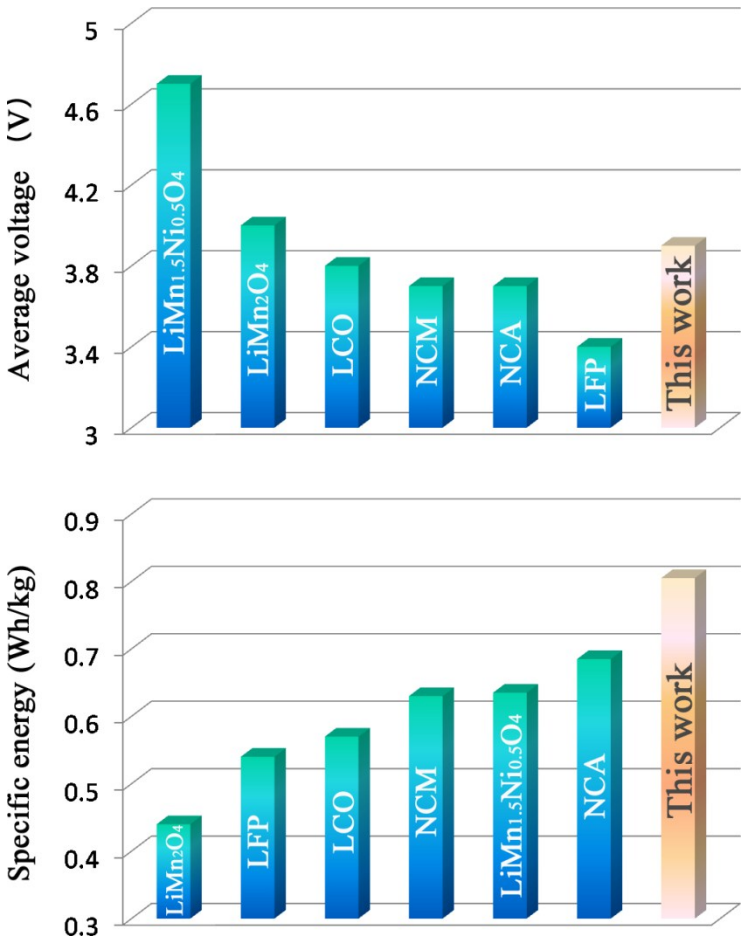

Figure S3. Comparisons of specific energy (kW h)/kg and working voltages vs. Li^+/Li for various cathode materials used as cathode for Li ion batteries.

High voltage spinel $LiMn_{1.5}Ni_{0.5}O_4$ shows a highest working voltage of 4.7 V, followed by $LiMn_2O_4$ of 4.0 V. Our material ranks the third of the various cathode materials of 3.9 V, highest among all the layered materials. Since the specific energy is determined by working voltage and capacity, the much higher capacity of the new material offsets the downside effect of slightly lower voltage than $LiMn_{1.5}Ni_{0.5}O_4$ and $LiMn_2O_4$, yielding a largest specific energy of 805 Wh/kg. Note its superior energy density retention, this novel material shows the promising applications in high-energy lithium ion batteries.

IV. Performance of 5-5 Li-rich oxide prepared using the similar preparation method

It is also worth noting that state-of-art's $0.5Li_2MnO_3 \cdot 0.5LiMO_2$ Li-rich oxides could deliver even higher capacity and specific energy but usually suffer from fatal voltage degradation, making this kind of material impractical for commercial use. Within similar synthesis method, we prepared one of most common 5-5 Li-rich oxide, $Li_{1.20}Mn_{0.54}Co_{0.13}Ni_{0.13}O_2$, and found that retention of specific energy over 60 cycles was as low as 80%, although the discharge capacity is well retained (Figure S4).

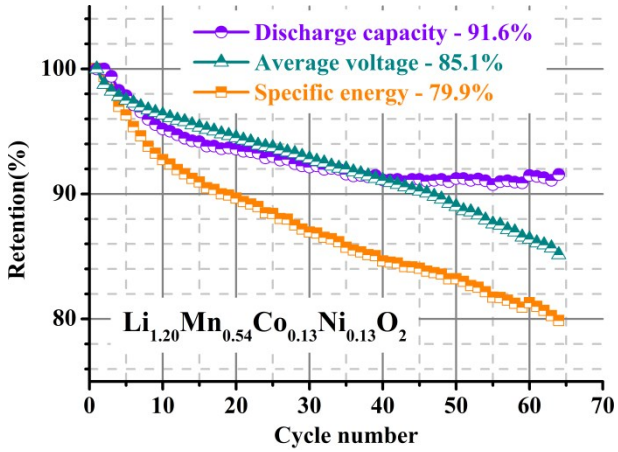

Figure S4. Retention values as a function of cycle numbers for common 5-5 Li-rich oxides $Li_{1.20}Mn_{0.54}Co_{0.13}Ni_{0.13}O_2$ ($0.5Li_2MnO_3 \cdot 0.5LiMn_{1/3}Co_{1/3}Ni_{1/3}O_2$) prepared using the similar synthesis method.

Discharge capacity is well retained over 65 cycles at same current density of 20 mA/g. However, average voltage decreases almost linearly to 85.1% at the end of cycling. More unfortunately, specific energy retains merely 79.9%, much inferior to the current novel composition reported in this work.

V. Galvanostatic intermittent titration technique (GITT) test

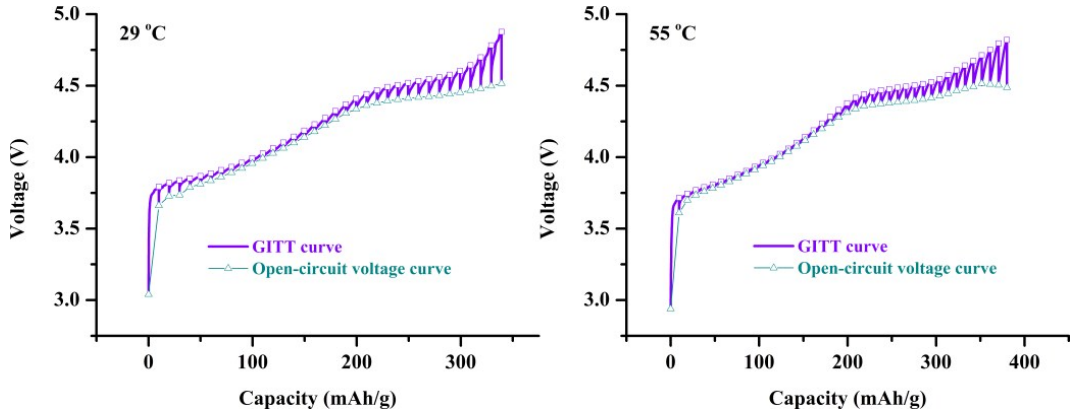

Figure S5. GITT curves recorded at 29 °C and 55 °C of $Li_{1.080}Mn_{0.503}Ni_{0.387}Co_{0.030}O_2$. GITT results were obtained by charging the cells with a constant current (CC) at 10 mA/g for 1 h and then cutting off the current for 5 h to reach a near-equilibrium state, and repeating until cut-off voltage (4.8 V) was reached.

The galvanostatic intermittent titration technique (GITT) is an useful tool to study the reaction kinetics at various states of charge. The voltage difference between the end of each interrupted CC charge (square) and the end of relaxation (triangle), defined as the overpotential, can be used as an indicator of the kinetics: larger the overpotential implies poorer kinetics.[2]

It can be seen from Figure S5 that the overpotential values below 4.4 V reamin low for the cell tested at 55 °C, while the values are larger for the one tested at 29 °C. This means that in this section, higher ambient temperature facilitates reaction kinetics, in consistent with CV, EIS analyses.

VI. Tentative experimental results regarding Li_2MnO_3 activation

To prove that Li_2MnO_3 activation is dependent on composition and temperature for Li-rich layered oxide, we intend to fix the Li_2MnO_3 and $LiMO_2$ ratio, while tuning the composition of $LiMO_2$ component of $xLi_2MnO_3 \cdot (1\text{-}x)LiMO_2$, and thereafter exert different temperatures to check the variation in electrochemical behavior. dQ/dV profiles of a group of Li-rich oxide are provided in Figure S6.

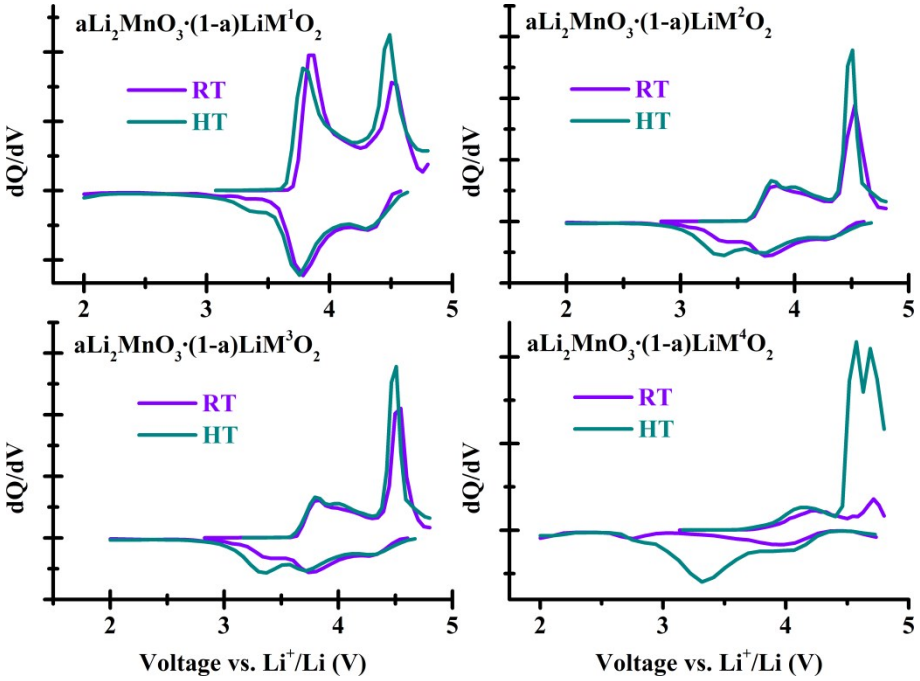

Figure S6. dQ/dV profiles of a group of Li-rich layered oxides, calculated from the initial charge/discharge data obtained at room temperature (RT) and high temperature (HT) of 55 °C.

By comparison of RT and HT plots in each figure, it can be found that lower-potential peaks are almost overlapped where as the 4.5 V peak is largely enhanced at HT, and a new peak below 3.6 V appears on the HT discharge branch for each composition. This is in good agreement with the analysis of Figure 8. Therefore, it could be concluded that electrochemical behavior (particularly the capacity) of $LiMO_2$ part, precisely Ni/Co redox, is temperature-independent. In a sharp contrast, electrochemical behavior of Li_2MnO_3 (activation) is highly temperature-dependent.

By comparing the RT branches among the four different compositions, it can be found that the relative ratio between two peaks on the charge branch is largely different. This indicates that the

degree of Li_2MnO_3 activation is also relevant to the composition of $LiMO_2$ end member. As a result, battery design can be achieved through composition tuning in $xLi_2MnO_3 \cdot (1\text{-}x)LiMO_2$.

VII. Evidence for formation of MO_2

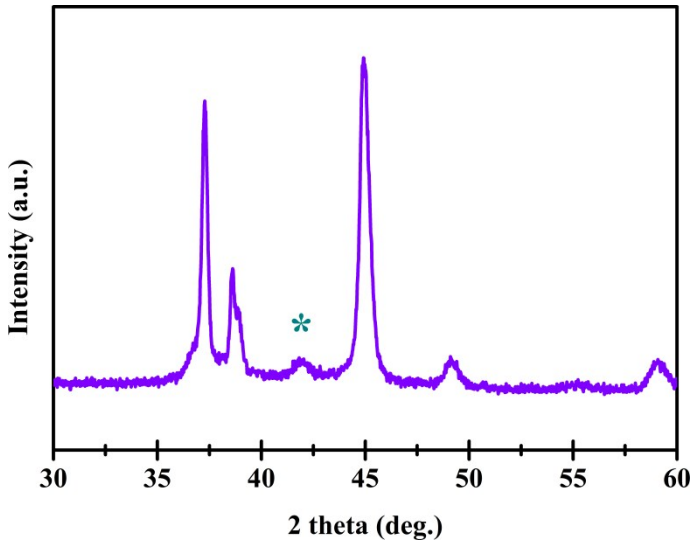

Figure S7. Ex-situ XRD of an electrode laminiate disassembled after charging to 4.8 V at 20 mA/g at 29 ^{o}C.

To detect the strucutre of the delithiated material, an ex-situ XRD of a charged electrode was recorded and shown in Figure S7. The newly appeared diffraction peak marked by symbol *, similar with that previously reproted,[3] indicate the formation of MnO_2.

Formation of "layered MO_2" is mainly based on electrochemistry of Li-rich layered cathodes and has been reported previously:

(1) $x\mathrm{LiMO_2}\cdot(1\text{-}x)\mathrm{Li_2MnO_3} \rightarrow x\mathrm{MO_2}\cdot(1\text{-}x)\mathrm{Li_2MnO_3}$

(2) $x\mathrm{MO_2}\cdot(1\text{-}x)\mathrm{Li_2MnO_3}\mathrm{MO_2}\cdot\mathrm{Li_2MnO_3} \rightarrow \mathrm{MO_2}\cdot\mathrm{MnO_2}$

VIII. Lowering upper limit of voltage

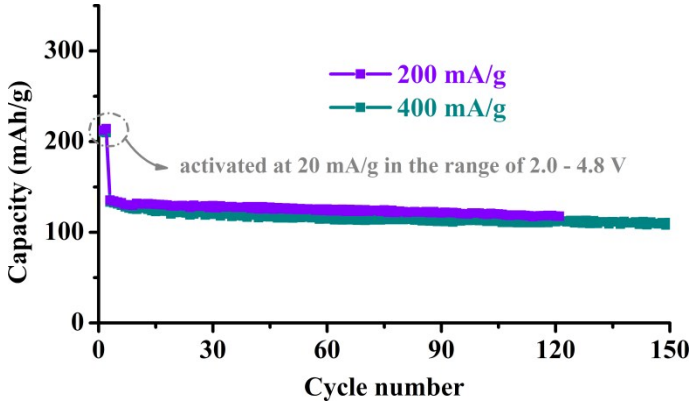

Figure S8. Cycling performance in the voltage range of 2.5 – 4.6 V at the rates of 200 and 400 mA/g.

In the voltage range of 2.5 to 4.6 V, our layered oxides showed an excellent cycling stability at each rate. Raising the voltage range to 4.8 V largely enhanced its capacity without sacrificing cycling stability.

IX. Lowering Li_2MnO_3 amount by reducing lithium source addition before sintering

To examine the stabilizing role of Li_2MnO_3 in $Li_{1.08}Mn_{0.503}Ni_{0.387}Co_{0.03}O_2$, we lowered the lithium concentration in the layered oxide to obtain a new composition of $Li_{0.98}Mn_{0.503}Ni_{0.38}Co_{0.03}O_2$ (determined by ICP results and normalized to Mn content 0.503). Its room temperature performance is shown in Figure S9a, along with Figure S9b of $Li_{1.08}Mn_{0.503}Ni_{0.387}Co_{0.03}O_2$ performance within the same range in question.

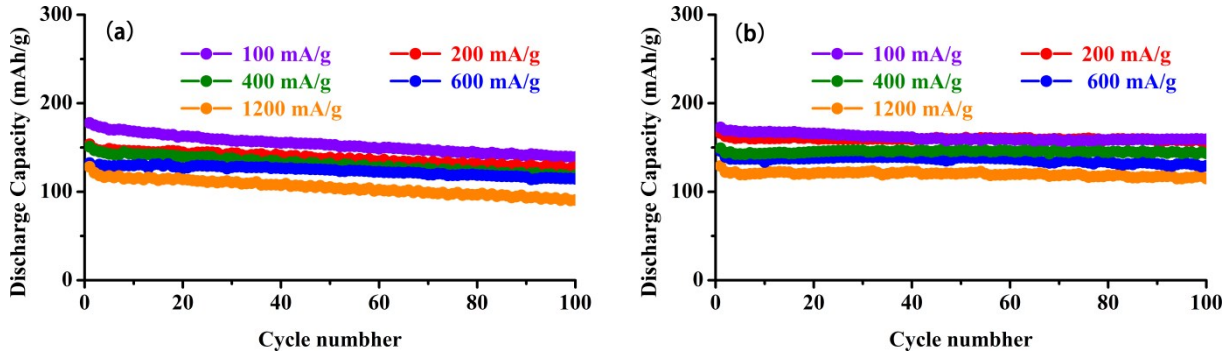

Figure S9. Cycling stability of (a) low-Li-concentration oxide $Li_{0.98}Mn_{0.503}Ni_{0.38}Co_{0.03}O_2$ and (b) $Li_{1.08}Mn_{0.503}Ni_{0.387}Co_{0.03}O_2$.

Through the comparison, it is self-evident that low Li_2MnO_3 oxide has inferior cycling stability than that shown in the context. For example, the capacity retention over 100 cycles at 100 mAh/g is 78%, whereas the high-Li-concentration oxide shows a retention as high as 94%.

X. Correlation between temperature, open-circuit voltage and voltage degradation

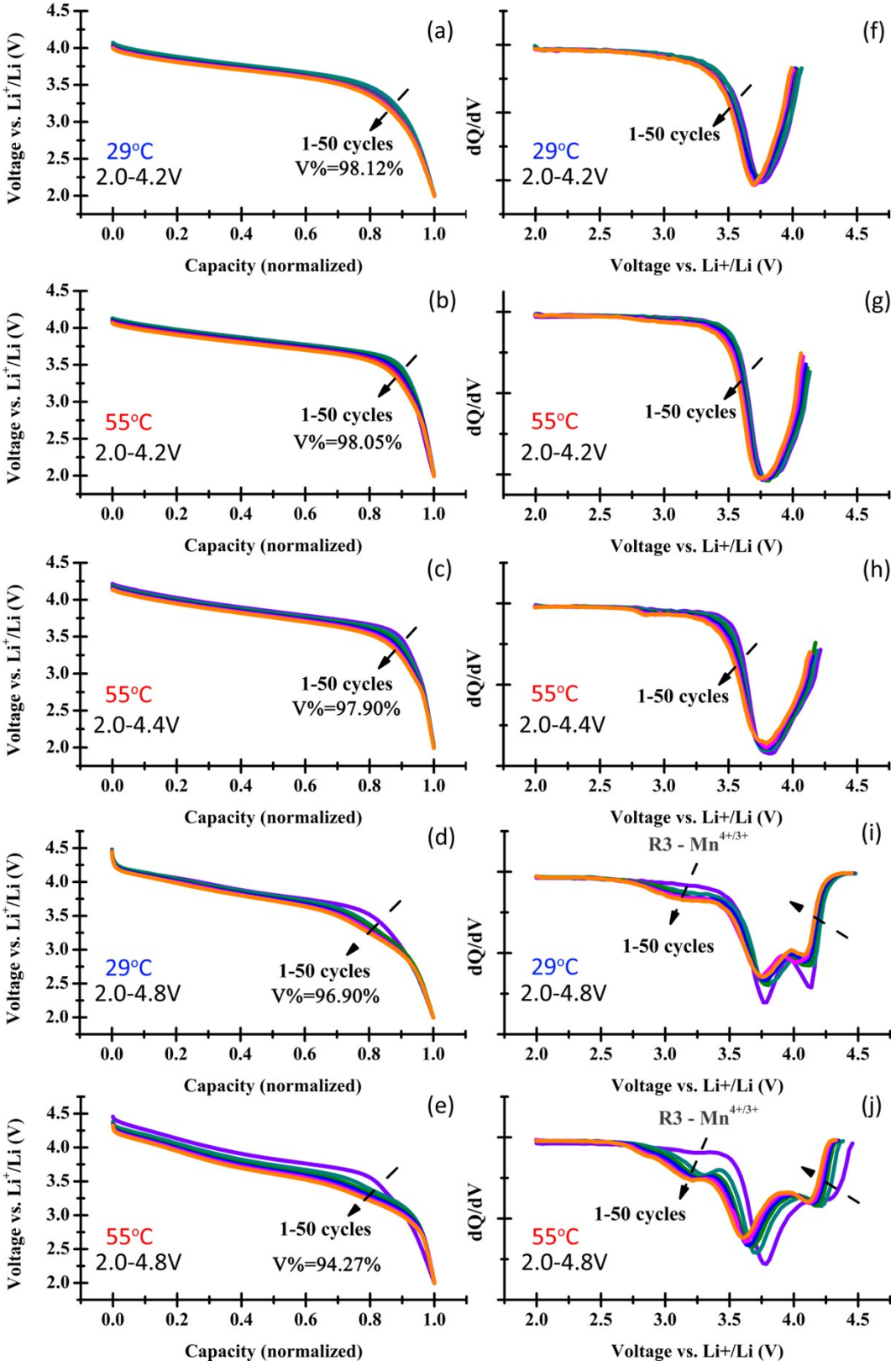

Figure S10. Normalized capacity discharge profiles at 200 mA/g and correspongding dQ/dV plots: (a, f) 2.0-4.2 V, 29 °C; (b, g) 2.0-4.2 V, 55 °C; (c, h) 2.0-4.4 V, 55 °C; (d, i) 2.0-4.8 V, 29 °C; (e, j) 2.0-4.8 V, 55 °C. V% stands for voltage retention.

To shed a light on the relationship between voltage fade and Li_2MnO_3 activation, a comparative experiment was conducted. In the experiment, Li_2MnO_3 activation (equals to the plateau region above 4.5 V), is controlled by tailoring the upper cut-off voltage (UCV) and ambient temperature. The results are shown in the form of normalized capacity discharge profiles in order to have a clear view of voltage fade upon cycling, and of dQ/dV plots to track the electrochemistry.

i. UCV < 4.5 V

UCV of 4.2 V is well below the activation voltage (4.5 V), and high voltage retentions are observed at both 29 ^oC and 55 ^oC (98.12% and 98.05%, respectively); when increasing UCV to 4.4 V, which is close to but still below the activation voltage, voltage rention is also high as 97.90%, very close to that of 4.2 V UCV. By monitoring their electrochemisty evolution during cycling by dQ/dV analysis, only one broad peak assigned to Ni/Co redoxes can be observed. It is understandable because at these UCVs, only $LiMO_2$-like region is electrochemically active, and Li_2MnO_3-like region is usually recogonized to be only active above 4.5 V. Note that voltage retention is shown to be irrespective to ambient temperature within this voltage limit. This is also in good agreement with our conclusion that temperature hardly influences Ni/Co redox in this material.

ii. UCV > 4.5 V

Further lifting the UCV to 4.8 V, which is well above activation voltage, the results show discrepancies in terms of ambient temperature. When working at 29 ^oC, it exhibited a high voltage retention of 96.90%, comparable to values at UCVs below 4.5 V; while a relatively low V% of 94.27% after 50 cycles was obtained at 55 ^oC. dQ/dV plots reveal their differences in electrochemistry: Mn^{4+}/Mn^{3+} redox couple is pronounced at 55 ^oC and contributes considerable portion to the overall capacity after cycling, thereby lowering the average voltage; on the contrary, although Mn^{4+}/Mn^{3+} redox is visible at 29 ^oC, but their low intensities lead to high voltage being well retained after cycling.

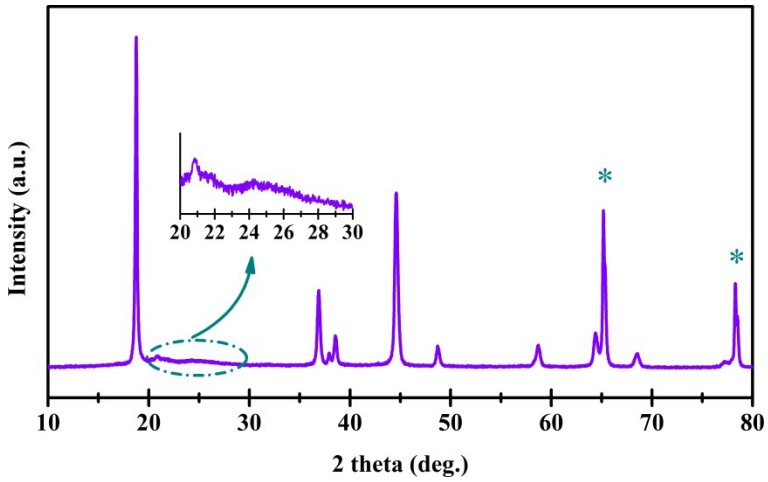

Figure S11. *Ex-situ* XRD pattern of $Li_{1.08}Mn_{0.503}Ni_{0.387}Co_{0.03}O_2$ after 50 cycles at 200 mA/g in the voltage range of 2.0-4.2 V at 55 °C. Symbol * represents for Al foil Bragg peaks.

To probe the average structure after cycling, an *ex-situ* XRD of the laminate disassembled after 50 cycles at UCV of 4.2 V was conducted and shown in Figure S11. The XRD pattern is almost unaltered when comparing with pristine laminate (bottom panel in Figure 9). Note that weak diffraction peaks between 20-30° is still observable, possibly due to that Li_2MnO_3 is not consumed at low UCV cycling. Note also that electrochemistry study clearly suggests inadequate Li_2MnO_3 activation (plateau chemistry) at 4.8 V UCV, 29 °C, therefore it is tempting to expect Li_2MnO_3 peaks showing up in its *ex-situ* XRD. The XRD pattern is reproduced from Figure 9 (middle panel) and shown in Figure S12. The 20-30° region is specifically enlarged, and indeed the weak peaks can be observed, though in rather low intensity when compared with that in Figure S11.

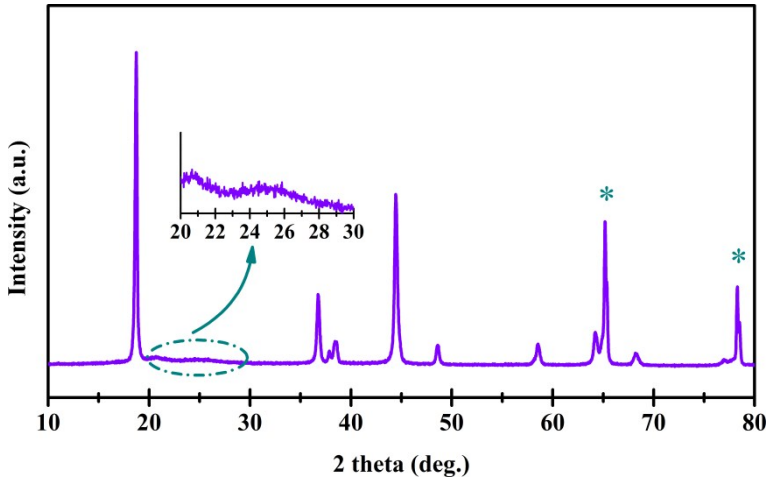

Figure S12. *Ex-situ* XRD pattern of $Li_{1.08}Mn_{0.503}Ni_{0.387}Co_{0.03}O_2$ after 50 cycles at 200 mA/g in the voltage range of 2.0-4.8 V at 29 °C. Symbol * represents for Al foil Bragg peaks.

To sum up, following conclusions can be obtained from above experiments:

(1) Serious voltage degradation occurs only when Li_2MnO_3 activation (equals to "plateau" chemistry) is fully reached;

(2) $Mn^{4+/3+}$ redox is derived from Li_2MnO_3 activation ("plateau" chemistry) and is responsible for voltage degradation upon cycling;

(3) Voltage fade can be mitigated by controlling Li_2MnO_3 activation ("plateau" chemistry) through tailoring UCV and/or ambient temperature (applicable when UCV > 4.5 V).

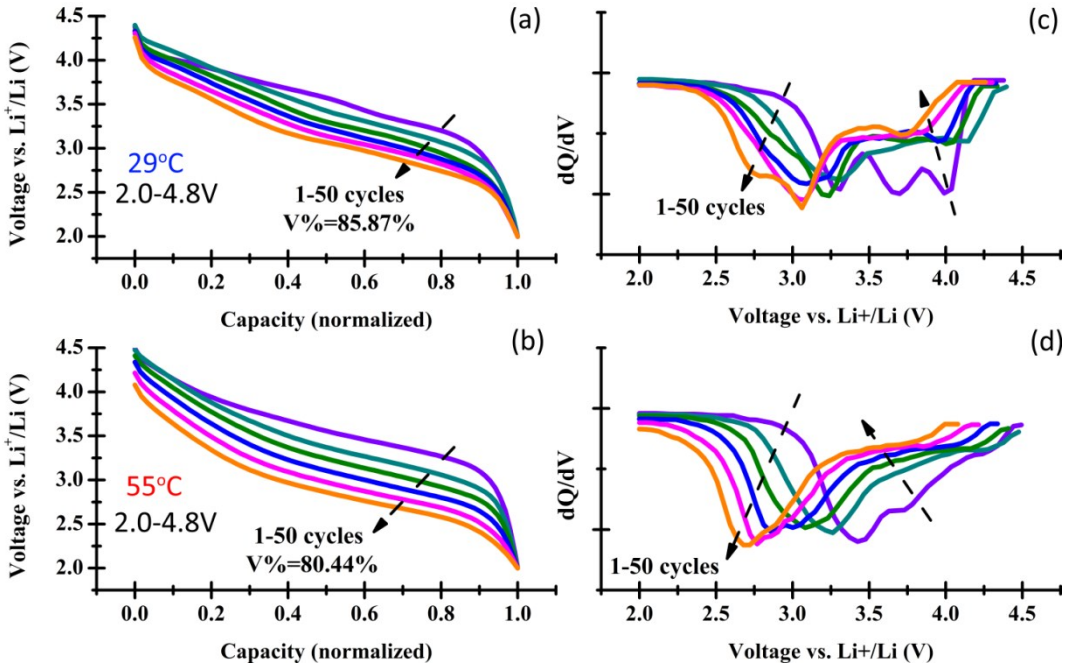

Figure S13. Normalized capacity discharge profiles at 200 mA/g and correspongding dQ/dV plots for 5-5 Li-rich oxides ($0.5Li_2MnO_3 \cdot 0.5LiMn_{1/3}Co_{1/3}Ni_{1/3}O_2$) prepared using the similar synthesis method: (a, c) 2.0-4.8 V, 29 °C; (b, d) 2.0-4.8 V, 55 °C. V% stands for voltage retention.

Note that in terms of room- or high- temperature LIBs, only those materials that are inadequately activated at room temperature (e.g., $Li_{1.080}Mn_{0.503}Ni_{0.387}Co_{0.030}O_2$) can be tuned by varing ambient temperature to deliever acceptable performances, in another word, there is no point for regulating temperatue for materials that are already over activated at room teperature (e.g. 5-5 Li-rich oxides).

In another experiment, a common 5-5 Li-rich oxide ($0.5Li_2MnO_3 \cdot 0.5LiMn_{1/3}Co_{1/3}Ni_{1/3}O_2$, or $Li_{1.20}Mn_{0.54}Co_{0.13}Ni_{0.13}O_2$) prepared with same method was subjected to both 29 °C and 55 °C cycling test at a rate of 200 mA/g, and the results are shown in Figure S13. This experiment aims (i) to highlight the advantage of the new composition of Li-rich oxide $Li_{1.08}Mn_{0.503}Ni_{0.387}Co_{0.03}O_2$, in terms of voltage retention and "tunable" voltage fade above room-temperature; and (ii) to demonstrate the

relationship between Mn redox with layered-to-spinel conversion. It is evident that for $Li_{1.20}Mn_{0.54}Co_{0.13}Ni_{0.13}O_2$, even at room temperature, Li_2MnO_3 activation process (the plateau region) is rather significant. This will certainly lead to large capacity contribution from $Mn^{4+/3+}$ redox and thus lowering its average voltage. Worsely, Mn redox peaks in the dQ/dV curve gradually evolves to 2.8 V peak due to the spinel conversion from layered structure. This greatly lowers the voltage retention, which is only 85.87% at 29 ^oC and low as 80.44% at 55 ^oC. In spite of decent capacity retention, its performance in voltage/energy retentivity is clearly against the application as room-temperature or high-temperature LIBs due to excessive activation.

References

[1] J. R. Croy, A. Abouimrane, Z. Zhang, *MRS Bulletin* 2014, **39**, 407.

[2] X. Yu, Y. Lyu, L. Gu, H. Wu, S.-M. Bak, Y. Zhou, K. Amine, S. N. Ehrlich, H. Li, K.-W. Nam, X.-Q. Yang, *Adv. Energy Mater.,* 2014*, DOI: 10.1002/aenm.201300950*

[3] C. Shen, Q. Wang, F. Fu, L. Huang, Z. Lin, S. Y. Shen, H. Su, X. M. Zheng, B. B. Xu, J. T. Li and S. G. Sun, *ACS Appl. Mater. Interfaces*, 2014, **6**, 5516-5524.

[4] S.-H. Kang and M. M. Thackeray, *Electrochem. Commun.*, 2009, **11**, 748-751.